Electronic Supplementary Material (ESI) for Journal of Materials Chemistry A.
This journal is © The Royal Society of Chemistry 2022

Electronic Supplementary Information

Boosted charge separation in direct z-scheme heterojunction of $CsPbBr_3$/ultrathin carbon nitride for improved photocatalytic CO_2 reduction

Fanqi Luo[a], Mingyang Liu[b], Mang Zheng[b], Qi Li*[b], Hong Wang*[a], Jing Zhou[c], Y ong Jiang[d], Yaoguang Yu[e], Baojinag Jiang*[a]

[a] F.Q. Luo, Prof. H. Wang, Prof. B. J. Jiang
Key Laboratory of Functional Inorganic Material Chemistry, Ministry of Education of the People' s Republic of China, School of Chemistry and Materials Science, Heilongjiang University, Harbin 150080, China.

[b] M. Y. Liu, M. Zheng, Q. Li
College of Material Science and Chemical Engineering, Harbin Engineering University, Harbin 150001, China.

[c] Prof. J. Zhou
Shanghai Institute of Applied Physics, Chinese Academy of Sciences, Shanghai 201800, China

[d] Prof.Y.Jiang
College of Biological and Chemical Engineering, Guangxi University of Science and Technology, Liuzhou 545006, China

[e] Prof. Y.Y. Yu
School of Materials, Sun Yat-sen University, Shenzhen 518107, P. R. China.
E-mail: liqchem@sina.com; wanghong1@hlju.edu.cn; jbj@hlju.edu.cn

Table of Content

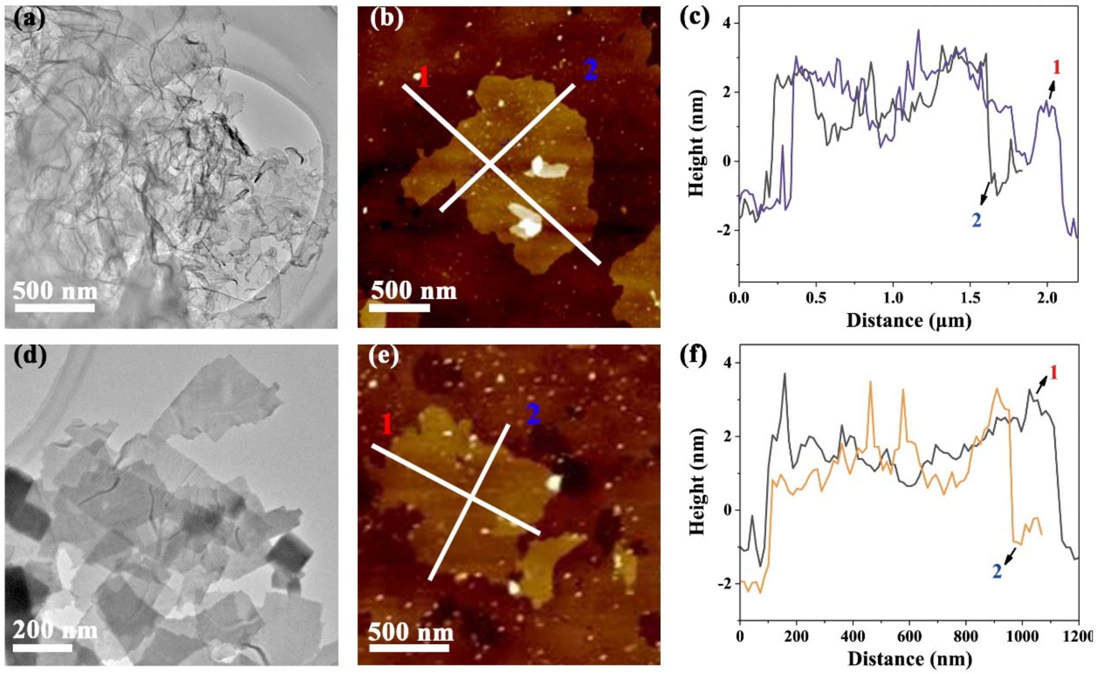

Fig. S1 Typical TEM, AFM images and height cutaway view of (a-c) CNN and (d-f) CPBN.

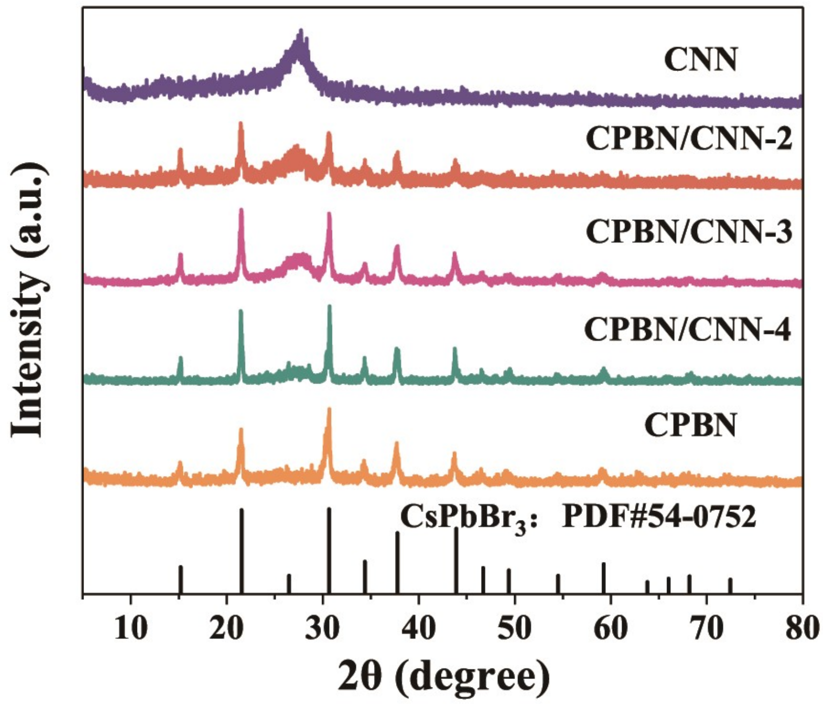

Fig. S2 XRD patterns of CPBN, CNN, CPBN/CNN-2, CPBN/CNN-3 and CPBN/CNN-4, respectively.

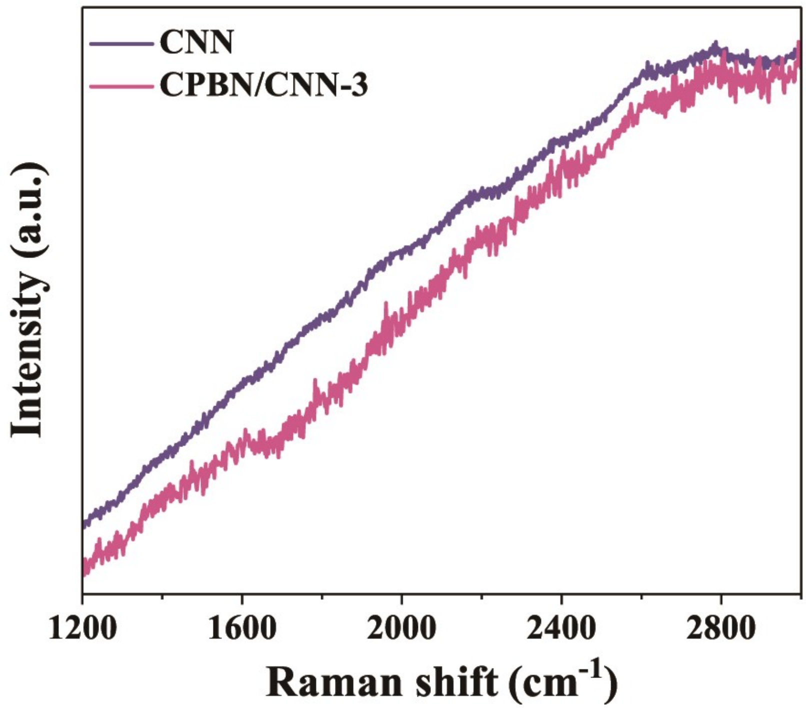

Fig. S3 Raman spectra of CNN and CPBN/CNN-3.

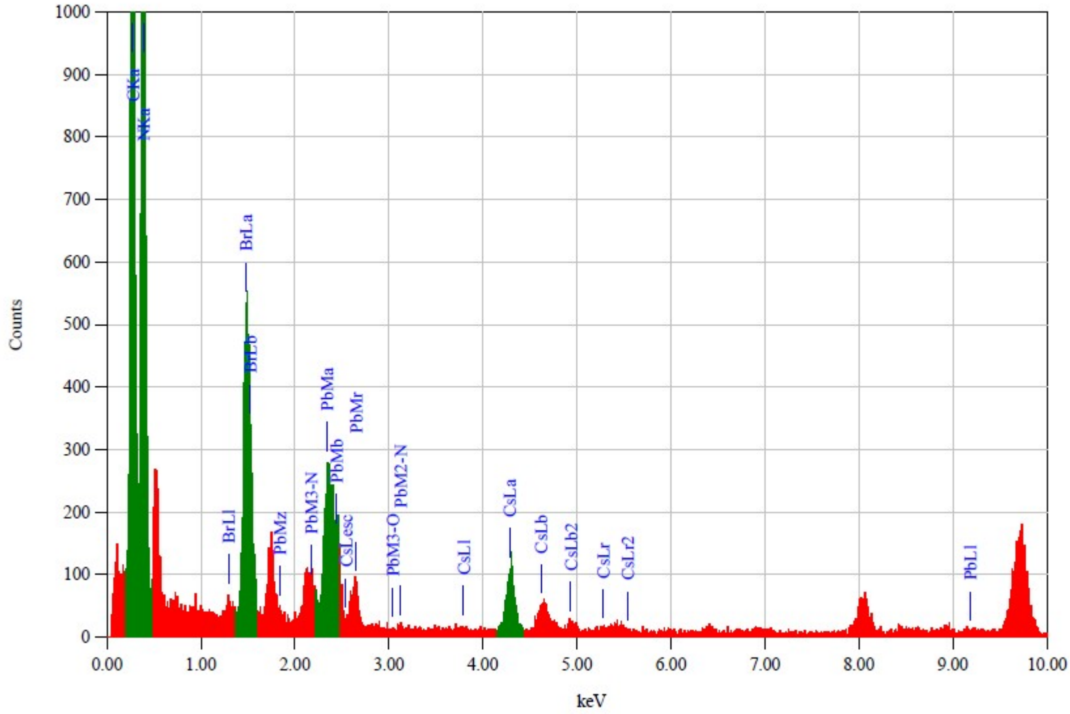

Fig. S4 EDX spectrum of CPBN/CNN-3.

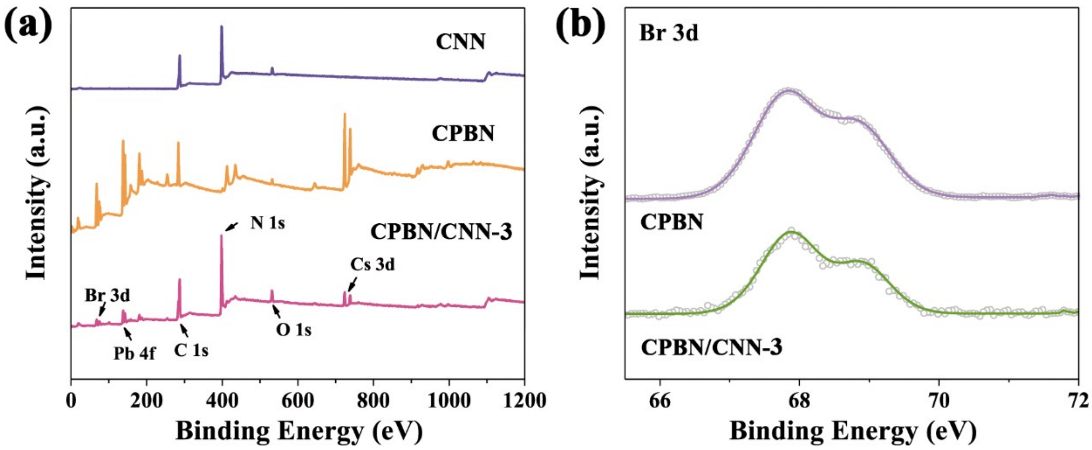

Fig. S5 The XPS spectra of samples: (a) survey, (b) Br 3d.

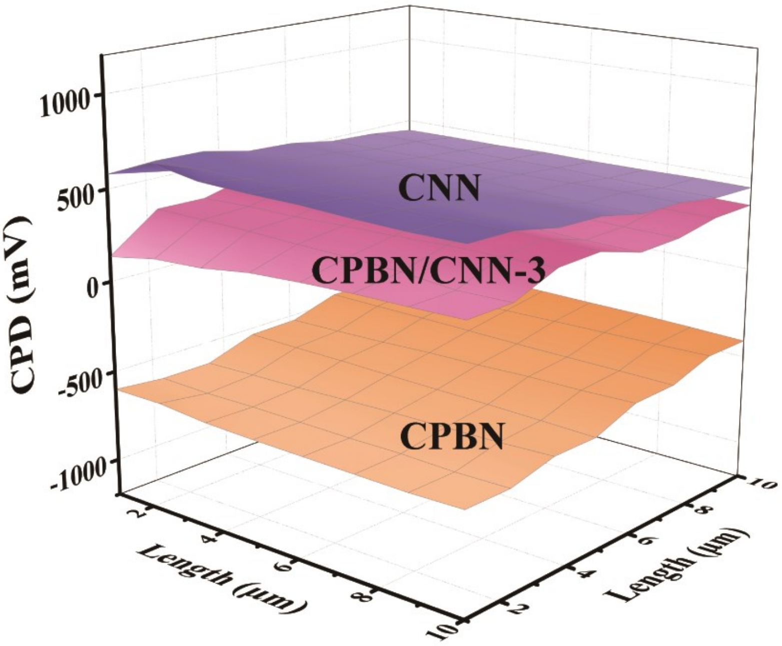

Fig. S6 Relative WF maps of CNN, CPBN and CPBN/CNN-3.

To further investigate the electron transfer between CNN and CPBN, the work function (WF) was measured using a Kelvin probe (Fig. S7). The results show that when CNN and CPBN are in contact, electrons are transferred from CPBN to CNN through the contact interface.

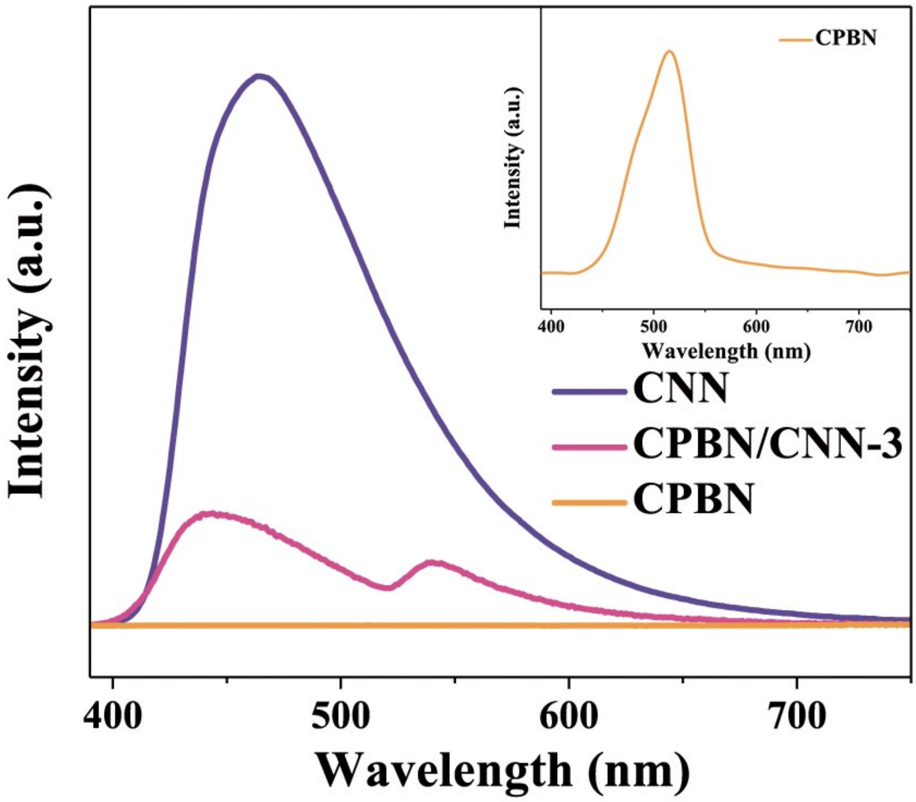

Fig. S7 Steady-state PL spectra of CNN, CPBN and CPBN/CNN-3.

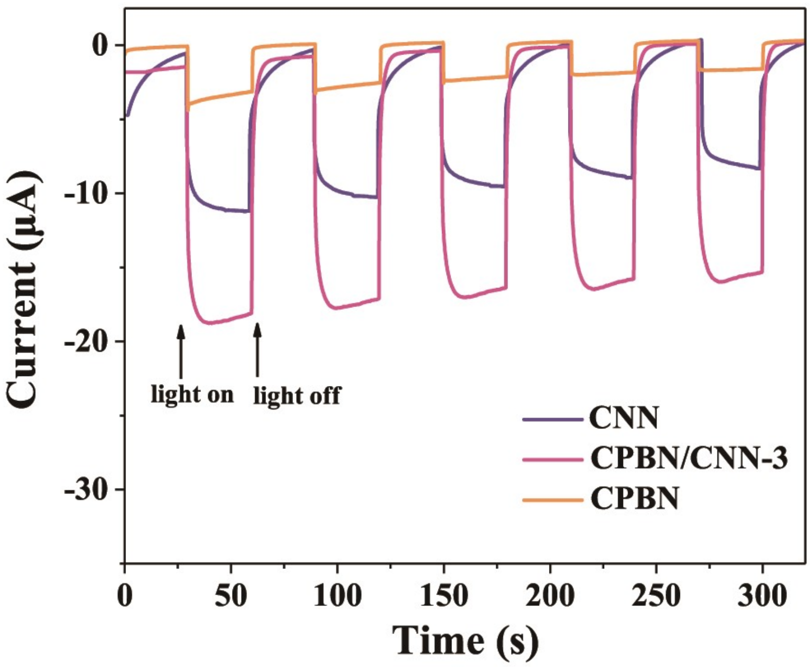

Fig. S8 Photoelectrochemical amperometric I-t plots of CNN, CPBN and CPBN/CNN-3.

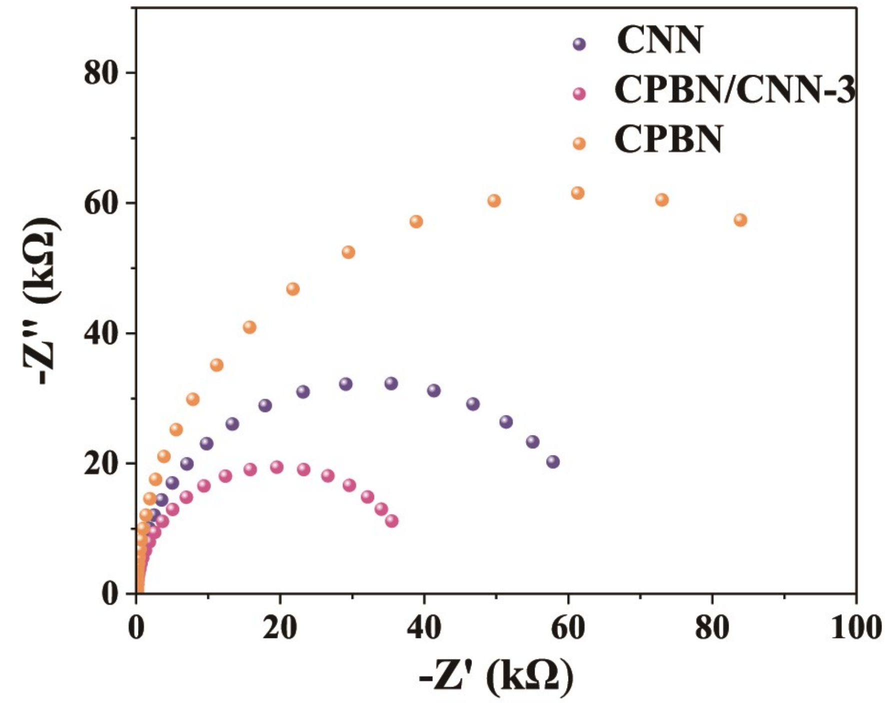

Fig. S9 EIS Nyquist plots of CNN, CPBN and CPBN/CNN-3.

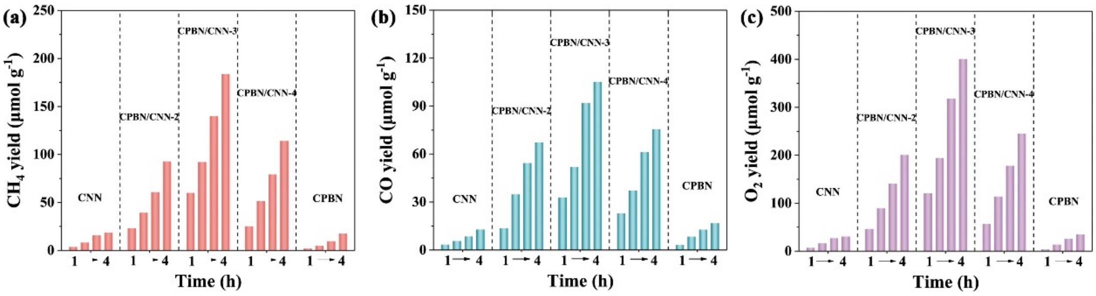

Fig. S10 (a) CH_4, (b) CO and (c) O_2 yield of CNN, CPBN and CPBN/CNN-X by recording every 1h upon illumination for 4 h.

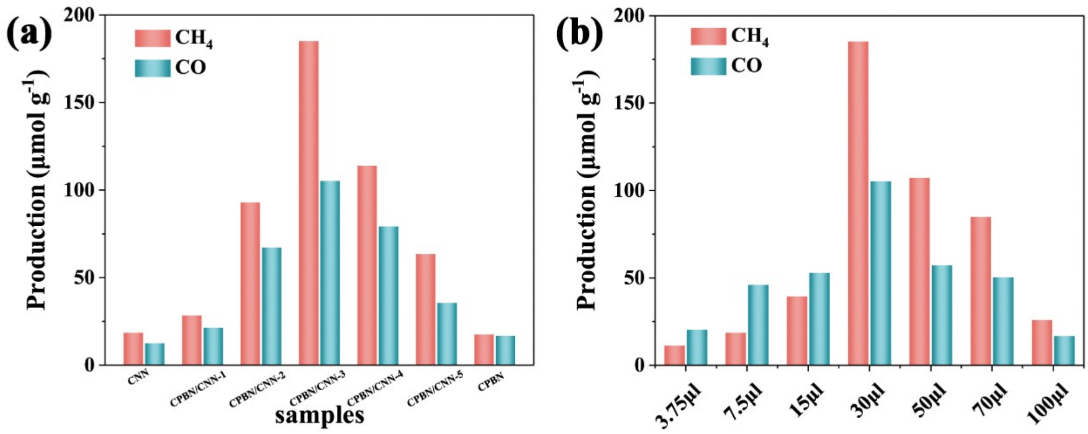

Fig. S11 (a) Photocatalytic time courses of, CO and CH_4 evolution of CNN, CPBN/CNN-X, CPBN, (b) CH_4 and CO yield of as-synthesized photocatalysts, along with different amount water.

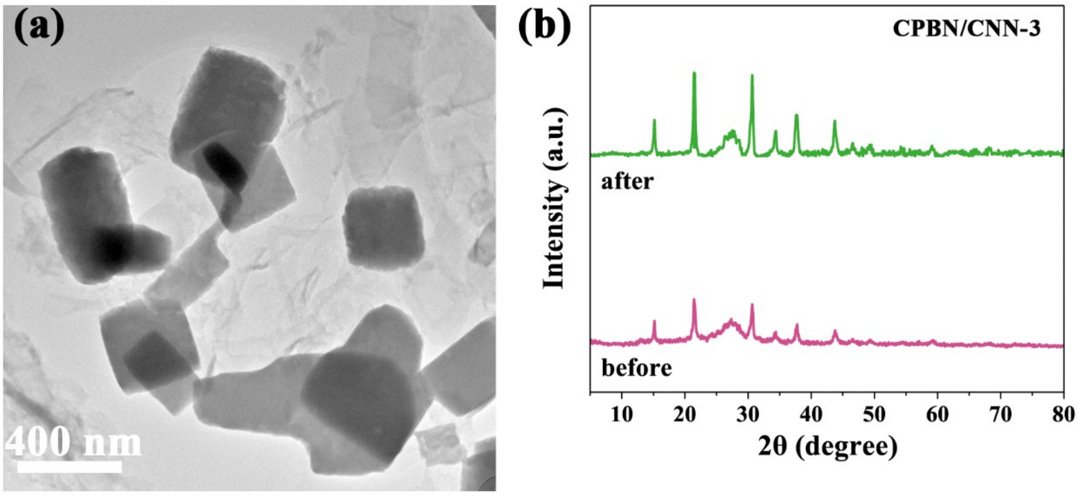

Fig. S12 (a) TEM and (b) XRD patterns of CPBN/CNN-3 after photocatalytic reaction.

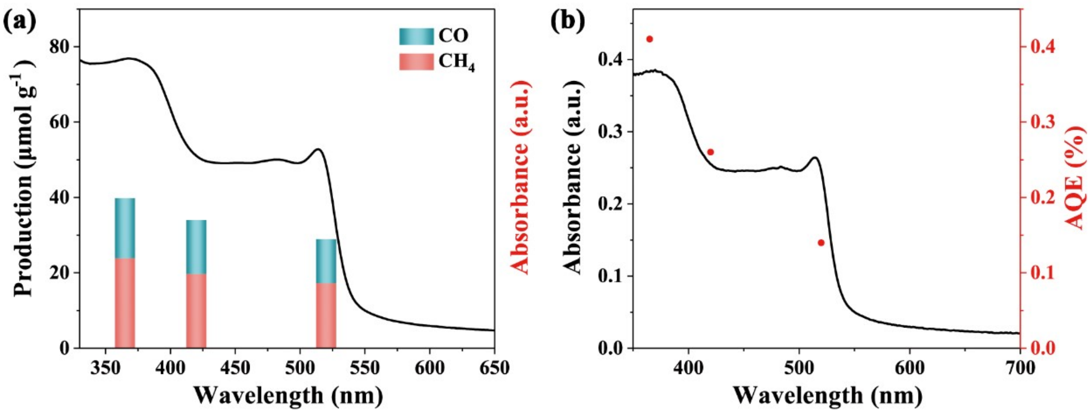

Fig. S13 The AQE of CPBN/CNN-3.

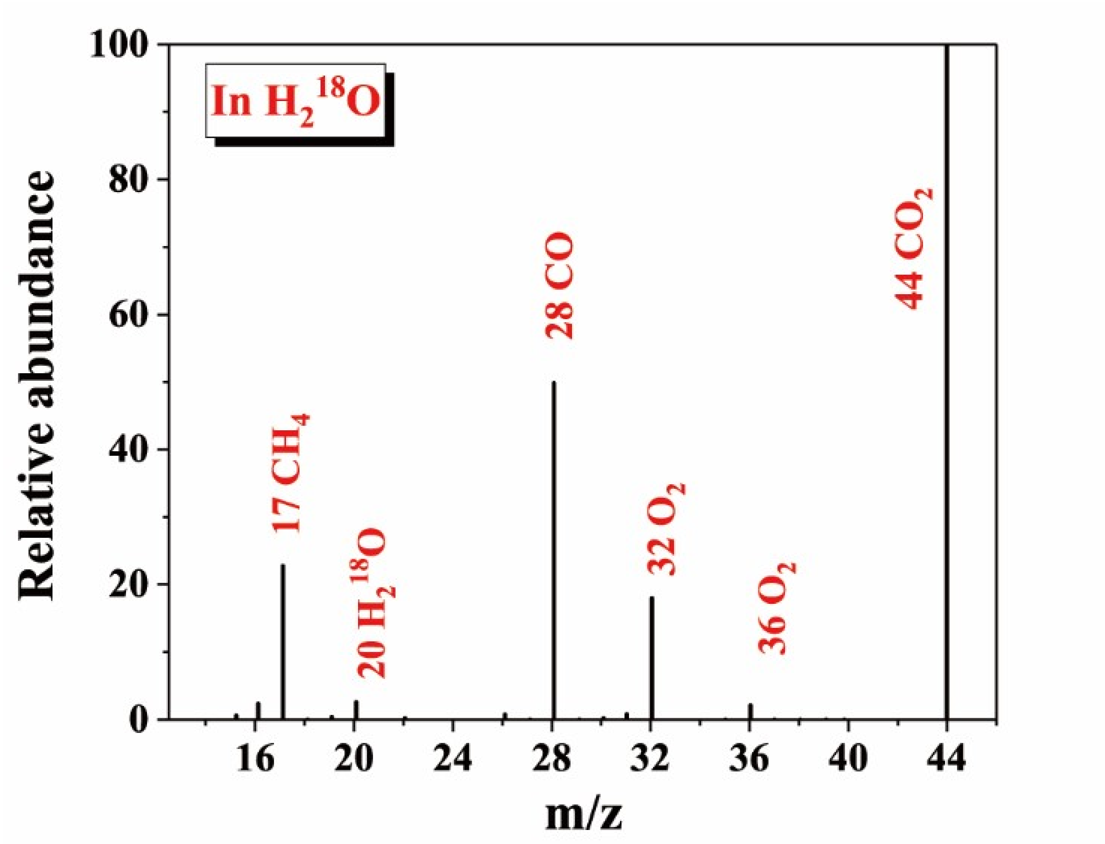

Fig. S14 (a) GC-MS spectrum of the gas-phase products driven for CPBN/CNN-3 in the photocatalytic reduction of $H_2{}^{18}O$.

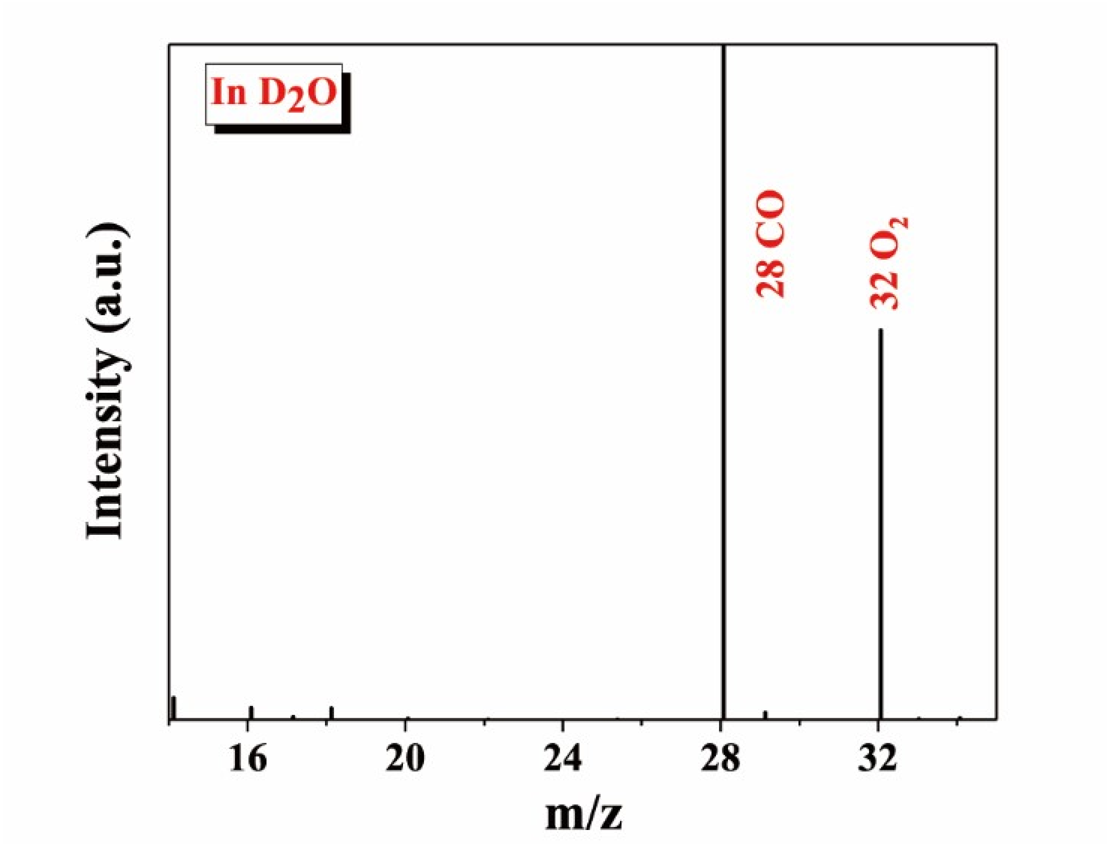

Fig. S15 GC-MS spectrum of the gas-phase products driven for CPBN/CNN-3 in the photocatalytic reduction of D_2O.

Table S1. Fitted PL decay parameters of CPBN， CNN and CPBN/CNN-3.

Sample	τ1/ns	A1/%	τ2/ns	A2/%	τ3/ns	A3/%	$\tau_{average}$/ns
CNN	3.13	37.58	12.58	42.92	67.52	19.51	14.63
CPBN	0.85	32.05	4.96	39.86	43.37	28.09	12.57
CPBN/CNN-3	3.28	34.22	13.69	41.49	93.64	24.29	23.73

Table S2. Summary of photocatalytic CO_2 reduction performances of different catalysts after irradiation for 4 h

Sample	Yieldco /μmol g^{-1}	$Yield_{CH4}$ /μmol g^{-1}	$Yield_{O2}$ /μmol g^{-1}	$Yield_{products}$ /μmol g^{-1}	$Yield_{electron}$ /μmol g^{-1} [a]	$R_{electron}$ /μmol g^{-1} h^{-1} [b]
CNN	12.9	15.3	30.6	28.2	148.2	37.1
CPBN/CNN-2	67.2	92.8	200.6	160.0	876.8	219.2
CPBN/CNN-3	105.2	184.0	398.3	289.2	1682.4	420.6
CPBN/CNN-4	79.2	114.0	245.0	193.2	1070.2	267.6
CPBN	16.8	17.6	35.4	34.4	174.4	43.6

The catalytic performances of samples were calculated according to the total weight of hybrid materials.

[a] The electron consumption yield was calculated with the following equation:

$Yield_{electron} = 2Yield_{CO} + 8Yield_{CH4}$

[b] The electron consumption rate was calculated with the following equation:

$R_{electron} = Yield_{electron} /4h$

Table S3. Comparison of the measured evolution rates of O_2 with its theoretical ones in terms of the amount of photoreduction products.

	Photoreduction product rate ($\mu mol\ g^{-1}\ h^{-1}$)	
	O_2 (theoretical)	O_2 (measured)
CNN	30.6	37.6
CPBN/CNN-2	200.6	219.2
CPBN/CNN-3	398.3	420.6
CPBN/CNN-4	245.0	267.6
CPBN	35.4	43.6

Table S4. Evolution of CO and CH_4 under different reaction conditions;

Sample	Condition	Yieldco /μmol g^{-1}	$Yield_{CH4}$ /μmol g^{-1}
CPBN/CNN-3	Ethyl acetate/water	105.2	184.0
CPBN/CNN-3	N_2	3.6	5.9
CPBN/CNN-3	Without light	0	0
CPBN/CNN-3	Ethyl acetate	21.78	5.7
No photocatalyst	Ethyl acetate/water	0	0

Table S5. Summary of the photocatalytic CO_2 reduction performance of perovskite-based catalysts.

Photocatalyst	Condition	Light source	Products /μmolg^{-1}h^{-1}	$R_{electron}$/ μmolg^{-1}h^{-1}	Ref	AQE
$CsPbBr_3$/GO	ethyl acetate	100W Xe Lamp AM1.5G 150Mw/cm^{-2}	CO,4.9 CH_4,2.5 H_2,0.13	29.8	1	-
$CsPbBr_3$-Re(CO)$_3$Br(dcbpy)	Toluene /isopropanol	150W Xe Lamp AM1.5G,>420nm 150Mw/cm^{-2}	CO,34.8 CH_4,1.9	73.4	2	-
$MAPbI_3$@PCN-221($Fe_{0.2}$)	ethyl acetate /water	300W Xe Lamp >400nm 100Mw/cm^{-2}	CO,4.2 CH_4,13	112	3	-
$CsPbBr_3$@ZIF-67	Gas (CO_2+H_2O)	100W Xe Lamp AM1.5G 150Mw/cm^{-2}	CO,0.8 CH_4,3.8	36.9	4	-
$CsPbBr_3$@ZIF-8	Gas (CO_2+H_2O)	100W Xe Lamp AM1.5G 150Mw/cm^{-2}	CO,0.5 CH_4,1.8	15.5	4	-
$CsPbBr_3$ NC /UIO-66(NH_2)	ethyl acetate /water	300W Xe lamp >420nm	CO,8.2 CH_4,0.3	18.5	5	-
$CsPbBr_3$ QD_S /PCN	acetonitrile/ water	300W Xe lamp >420nm	CO,148.9	297.8	6	-
$CsPbBr_3$ NC /a-TiO_2	ethyl acetate /isopropanol	150W Xe Lamp AM1.5G 150Mw/cm^{-2}	CO,3.9 CH_4,6.7 H_2,1.5	64.5	7	-
$CsPbBr_3$ NC /Pd NC	Gas (CO_2+H_2O)	150W Xe Lamp AM1.5G 150Mw/cm^{-2}	CO,1.9 CH_4,3.6 H_2,1.1	33.8	8	0.017% (420 nm)
$CsPbBr_3$@CN	ethyl acetate	450W Xe Lamp AM1.5G	CO,3.1 CH_4,22.9	189.4	9	-
Pt$CsPbBr_3$/ Bi_2WO_6	ethyl acetate/ isopropanol	150W Xe Lamp AM1.5G 100Mw/cm^{-2}	CO,17.2 CH_4,34.4 H_2,7.4	324.0	10	-

$CsPbBr_3$@TiO-CN	ethyl acetate /water	300W Xe lamp 100Mw/cm^{-2}	CO,12.9	25.8	11	-
$CsPbBr_3$ NCs /MXene-20	ethyl acetate	300W Xe Lamp >420nm	CO,26.6 CH_4,6.8	107.6	12	-
α-Fe_2O_3/Amine-RGO/$CsPbBr_3$	Gas (CO_2+H_2O)	150W Xe Lamp AM1.5G,>420nm 150Mw/cm^{-2}	CO,2.3 CH_4,9.4 H_2,0.3	80.7	13	-
$CsPbBr_3$ /USGO/α-Fe_2O_3	acetonitrile/water	300W Xe Lamp >400nm 100Mw/cm^{-2}	CO,73.8	147.6	14	-
$CsPbBr_3$ /BP	ethyl acetate /water	300W Xe Lamp 200Mw/cm^{-2}	CO,44.7 CH_4,10.7	175.0	15	-
$CsPbBr_3$ QD_S /Bi_2WO_6	ethyl acetate /water	>400nm 100Mw/cm^{-2}	CO+CH_4, 50.3	144.4	16	-
$FAPbBr_3$/ Bi_2WO_6	benzyl alcohol	150W Xe Lamp AM1.5G 100Mw/cm^{-2}	CO,170	340.0	17	1.2% (400 nm)
$CsPbBr_3$/C_3N_4	ethyl acetate /water	150W Xe Lamp AM1.5G 150Mw/cm^{-2}	CO,26.3 CH_4,46.0	420.6	This work	0.24% (420 nm)

References:

1. Y. F. Xu, M. Z. Yang, B. X. Chen, X. D. Wang, H. Y. Chen, D. B. Kuang and C. Y. Su, *J. Am. Chem. Soc.,* 2017, **139**, 5660 —5663.
2. Z.C. Kong, H.H. Zhang, J.F. Liao, Y.-J. Dong, Y. Jiang, H.Y. Chen and D.B. Kuang, *Solar RRL*, 2019, **4**, 1900365.
3. L.-Y. Wu, Y.-F. Mu, X.-X. Guo, W. Zhang, Z.-M. Zhang, M. Zhang and T.-B. Lu, *Angew. Chem., Int. Ed*., 2019, **58**, 9491 —9495.
4. Z.-C. Kong, J.-F. Liao, Y.-J. Dong, Y.-F. Xu, H.-Y. Chen, D.-B. Kuang and C.-Y. Su, *ACS Energy Lett.,* 2018, **3**, 2656 —2662.
5. S. Wan, M. Ou, Q. Zhong and X. Wang, *Chem. Eng. J.,* 2019, **358**, 1287 —1295.
6. M. Ou, W. Tu and S. Yin, et al., *Angew. Chem.,* 2018, **130**, 13758 —13762.
7. Y. F. Xu, X. D. Wang, J. F. Liao, B. X. Chen, H. Y. Chen and D. B. Kuang, *Adv. Mater. Interfaces,* 2018, **5**, 1801015.
8. Y.-F. Xu, M.-Z. Yang, H.-Y. Chen, J.-F. Liao, X.-D. Wang and D.-B. Kuang, *ACS Appl. Energy Mater.,* 2018, **1**, 5083 —5089.
9. S.-Q. You, S.-H. Guo, X. Zhao, M. Sun, C.-Y. Sun, Z.-M. Su and X.-L. Wang, *Dalton Trans.,* 2019, **48**, 14115 —14121.
10. Y. Jiang, H. Chen, J. Li, J. Liao, H. Zhang, X. Wang and D. Kuang, *Adv. Funct. Mater.,* 2020, **30**, 2004293.
11. X.-X. Guo, S.-F. Tang, Y.-F. Mu, L.-Y. Wu, G.-X. Dong and M. Zhang, *RSC Adv.,* 2019, **9**, 34342 —34348.
12. A. Pan, X. Ma, S. Huang, Y. Wu, M. Jia, Y. Shi, Y. Liu, P. Wangyang, L. He and Y. Liu, *J. Phys. Chem. Lett.,* 2019, **10**, 6590 —6597.
13. Y. Jiang, J. Liao, H. Chen, H. Zhang, J. Li, X. Wang and D. Kuang, *Chem,* 2020, **6**, 766 —780.
14. Y. F. Mu, W. Zhang, G. X. Dong, K. Su, M. Zhang and T. B. Lu, *Small,* 2020, **16**, e2002140.
15. X. D. Wang, J. He, J. Y. Li, G. Lu, F. Dong, T. Majima and M. S. Zhu, *Appl. Catal., B,* 2020, **277**, 119230.
16. J. Wang, J. Wang, N. Li, X. Du, J. Ma, C. He and Z. Li, *ACS Appl. Mater. Interfaces*, 2020, **12**, 31477 —31485.
17. H. Huang, J. Zhao, Y. Du, C. Zhou, M. Zhang, Z. Wang, Y. Weng, J. Long, J. Hofkens, J. A. Steele and M. B. J. Roeffaers, *ACS Nano*, 2020, **14**, 16689 —16697.